Chemical Science

RSC Publishing

EDGE ARTICLE

View Article Online
View Journal | View Issue

Cite this: *Chem. Sci.*, 2013, **4**, 4426

A dinuclear iridium(III) complex as a visual specific phosphorescent probe for endogenous sulphite and bisulphite in living cells†

Guanying Li,[a] Yu Chen,[a] Jinquan Wang,[a] Qian Lin,[a] Jing Zhao,[b] Liangnian Ji[a] and Hui Chao*[a]

Received 16th August 2013
Accepted 2nd September 2013

DOI: 10.1039/c3sc52301b

www.rsc.org/chemicalscience

A non-emissive dinuclear iridium(III) complex (**SP-2**) linked *via* an azo group has been adopted as a phosphorescent probe for sulphite and bisulphite. **SP-2** exhibits a turn-on phosphorescent response toward sulphite and bisulphite with high selectivity and sensitivity. Furthermore, this probe can be used for living cell imaging to identify the presence of both external sulphite/bisulphite supplemented into cell cultures and endogenous sulphite/bisulphite biosynthesised in living cells.

Introduction

Sulphur dioxide (SO_2) is a common gaseous environmental pollutant. Inhaled SO_2 can be rapidly hydrated to sulphite and bisulphite and may cause airway diseases[1] (such as chronic bronchitis, asthma, and emphysema) and even lung cancer.[2] Sulphite, which has antioxidant and preservative properties, is used in food to prevent unpleasant browning, in wines to discourage bacterial growth, and in pharmaceuticals to maintain the stability and potency of some medications.[3] Normally, the ratio of sulphite to bisulphite is 3 : 1 (M/M) in neutral fluid and plasma, and the reference concentration for total serum sulphite is 0–9.85 μM in healthy donors.[4] In patients with acute pneumonia and chronic renal failure, however, the serum sulphite concentration significantly increases.[5] In addition, sulphite and bisulphite can also be generated endogenously from sulphur-containing amino acids, such as L-cysteine, or from thiosulphate in mammals and can play an important role in the biological sulphur cycle in the body.[6] Sulphite and bisulphite have toxicological effects at high concentrations, but at physiological or low concentration, they may have a physiological role in the regulation of cardiovascular function, separate from the toxicological effects. Studies have suggested that sulphite and bisulphite have vasodilating effects and elicit a dose-dependent negative inotropic effect.[7]

The biological effects of sulphite and bisulphite are now beginning to be understood; however, a large number of their effects remain unknown. One bottleneck may be the lack of convenient methods for accurately measuring the sulphite/bisulphite concentrations in biological systems. Some methods are available for sulphite/bisulphite determination *in vitro*, such as titrimetry, flow injection analysis, capillary electrophoresis, ion chromatography, gas chromatography and spectrophotometry.[3] Currently, the most common method for determining sulphite/bisulphite levels in biological samples, such as blood or tissues, is a high-performance liquid chromatographic (HPLC) assay.[5,8] However, some of these methods require complicated instruments and skilled personnel. Furthermore, they all suffer from troublesome sample pre-treatment and reagent preparation, which is time-consuming and unsuitable for measuring biological samples subject to rapid metabolism. A real-time analysis method for biological sulphite/bisulphite determination would be valuable.

After decades of development, fluorescent molecular probes possessing high spatial and temporal resolution have become powerful tools for chemists and biologists in combining chemical determination and real-time biological mapping. Recently, many fluorescent probes have been successfully developed for monitoring ions,[9] small molecules[10] and biomacromolecules[11] inside living cells. Only a few fluorescent molecular probes for sulphite or bisulphite have been reported *via* the functionalisation of an aldehyde group[12] or levulinate ester.[13] These fluorescent probes are mainly focused on *in vitro* assays due to the limitations of working conditions, high background signal and the potential interference from biological species. For example, the aldehyde-based probes may react with mercapto groups or amino groups in proteins, and the levulinate ester may be cleaved by esterase. These facts hinder their use in biological sulphite/bisulphite determination. Recently, an aldehyde-based fluorescent probe (**P-1**, Scheme 1)[14] was developed for bioimaging bisulphite in Hela cells, ignoring the fact that this probe had been used as a thiol probe,[15] and

[a]*MOE Key Laboratory of Bioinorganic and Synthetic Chemistry, State Key Laboratory of Optoelectronic Materials and Technologies, School of Chemistry and Chemical Engineering, Sun Yat-Sen University, Guangzhou, 510275, China. E-mail: ceschh@mail.sysu.edu.cn*

[b]*School of Chemical Biology and Biotechnology, Peking University, Shenzhen 518055, China*

† Electronic supplementary information (ESI) available. Fig. S1–S14 and Table S1. See DOI: 10.1039/c3sc52301b

there are millimolar concentrations of thiols found inside most cells.[10b] Another probe, with an α,β-unsaturated coumarin-hemicyanine dye (**P-2**, Scheme 1),[16] was synthesised and used for probing and imaging sulphite/bisulphite in Hela cells that were supplemented into cell cultures exogenously. However, until now, no probe for imaging endogenous sulphite/bisulphite in living cells was available. Herein, we report a phosphorescent off–on responsive probe for biological sulphite/bisulphite in both *in vitro* assays and intracellular imaging. In addition, this probe can also quantify the enzymatically generated sulphite and bisulphite inside cells. To the best of our knowledge, this is the first example of the imaging of endogenous sulphite and bisulphite in living cells.

Results and discussion

Design and synthesis

Azo compounds can be degraded by strong reducing agents, such as sodium dithionite. When an azo group is incorporated into transition metal complexes, such as ruthenium(II), osmium(III), rhenium(I) and zinc(II) complexes, it can be activated by the metal and become more reactive.[17] More importantly, the azo group is electron-withdrawing and can quench the luminescence efficiency of luminescent metal complexes by trapping electrons in the metal-to-ligand charge-transfer (MLCT) excited state.[17c] Therefore, the destruction of an azo group triggers a change in the electronic properties and thus the luminescent properties of metal complexes. Compared with other transition metal complexes, cyclometalated iridium(III) complexes have electronic properties and charge-transfer characteristics that can be tuned over wide ranges by choosing an appropriate ligand.[18]

With this in mind, we synthesised mono- and di-nuclear cyclometalated iridium(III) complexes bridged *via* an azo group, $[Ir(ppy)_2(azobpy)]^+$ (**SP-1**) and $[Ir(ppy)_2(azobpy)Ir(ppy)_2]^{2+}$ (**SP-2**) (ppy = 2-phenyl-pyridine, azobpy = 4,4′′-azobis(2,2′-bipyridine), Scheme 1), and examined their reactivity with sulphite and bisulphite. The syntheses were simple, and good yields were obtained from the one step reaction of $Ir_2(ppy)_4Cl_2$[19] with the azobpy ligand[20] in a 1 : 1 solution of $CH_3OH/CHCl_3$. For the mononuclear complex **SP-1**, an excess amount of azobpy ligand was needed to ensure that only the monoiridium centre was coordinated. For the dinuclear complex **SP-2**, a stoichiometric ratio of $Ir_2(ppy)_4Cl_2$ and azobpy were mixed and reacted in $CH_3OH/CHCl_3$ (1 : 1, v/v) under reflux for 4 h. The crude products were purified by aluminium oxide chromatography with $CHCl_3$ and CH_3OH as the eluents. These complexes were characterised by elemental analysis, ESI-MS and ^1H NMR spectra.

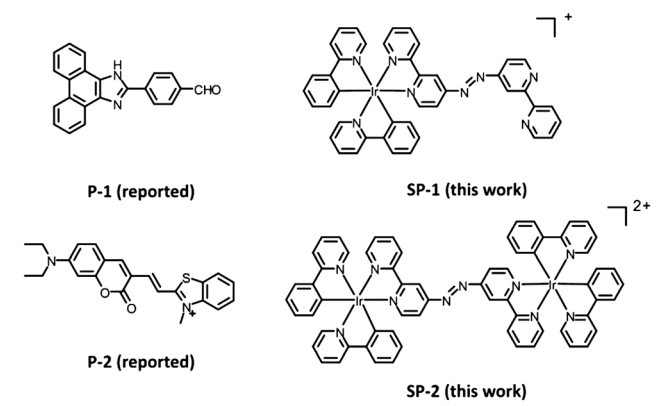

Scheme 1 Examples of sulphite and/or bisulphite probes.

Phosphorescent response toward sulphite/bisulphite

We first tested the phosphorescent response toward sulphite and bisulphite of **SP-1**. **SP-1** was weakly phosphorescent. Upon the addition of 100 μM sulphite or bisulphite into a 10 μM **SP-1** solution in a mixed solution of DMSO : HEPES buffer (3 : 7, 10 mM, pH 7.5), a minimal enhancement in the phosphorescence intensity was observed (ESI, Fig. S1†). The physiological concentration of total sulphite was detected from 10^{-6} to 10^{-4} M in different tissues and blood samples.[4,5,8] Therefore, **SP-1** is not suitable for biological sulphite determination.

When **SP-2** reacted with sulphite, however, a remarkable enhancement of phosphorescence intensity was observed (Fig. 1). **SP-2** (10 μM) in a mixed solution of DMSO : HEPES buffer (3 : 7, 10 mM, pH 7.5) was treated with increasing concentrations of sodium sulphite (0–30 μM), and then the emission spectra were recorded at 405 nm excitation after 3 min. The phosphorescence intensity increased linearly with the concentration of sulphite up to 10 μM ($R = 0.999$) and then reached a plateau. A similar situation was found when **SP-2** reacted with bisulphite (ESI, Fig. S2†). The phosphorescence signal showed a 26-fold enhancement for sulphite and a 27-fold enhancement for bisulphite. The calibration curves were set to determine the detection limit of sulphite (or bisulphite) with a 3 : 1 signal/noise ratio[21] (ESI, Fig. S3†). The detection limit was calculated as 0.24 μM for sulphite and 0.14 μM for bisulphite (ESI, Table S1†) *in vitro* assays. When **SP-2** was reacted with 10 μM sulphite, the phosphorescence intensity reached a plateau in approximately 2 min (Fig. 2). The phosphorescent response of

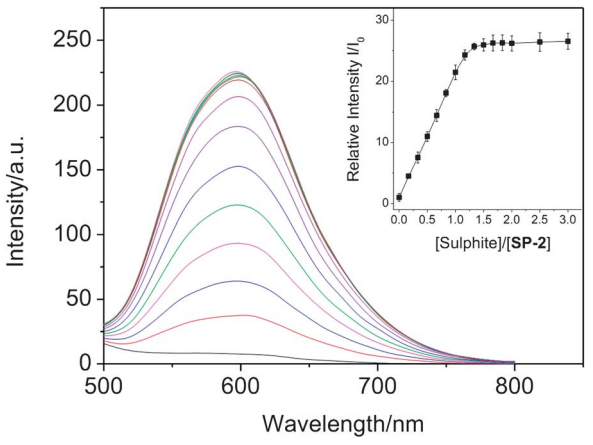

Fig. 1 Emission spectra of **SP-2** (10 μM) treated with increasing concentrations of sulphite (0–30 μM) in a mixed solution of DMSO : HEPES buffer (3 : 7, 10 mM, pH 7.5). Inset: the titration curve of **SP-2** reacted with sulphite. Each spectrum was recorded at 405 nm excitation.

SP-2 toward sulphite was dose-dependent and rapid. The ultimate enhancements in phosphorescence intensity show little difference between sulphite and bisulphite. However, the reaction rate of **SP-2** with bisulphite was faster than that with sulphite. The observed rate constants (k) at 10 μM bisulphite or sulphite were determined using the rate law $\ln(I/I_0) = kt$, where I and I_0 are the phosphorescent intensity of **SP-2** reacted with bisulphite or sulphite at the time of 0 and t second, and t represents time. The k value was calculated as $(0.177 \pm 0.011)\ S^{-1}$ for bisulphite, and $(0.107 \pm 0.004)\ S^{-1}$ for sulphite (ESI, Fig. S4†). More importantly, the pH titration curve revealed that the phosphorescence intensity was barely affected when the pH was varied from 4–10 (ESI, Fig. S5†). The data demonstrated that **SP-2** is effective at physiological pH with little variation. The off–on and fast response of the phosphorescence signal intensity support the use of **SP-2** as a sulphite/bisulphite probe.

We further examined the specificity of **SP-2** for sulphite by measuring its phosphorescence intensity after the addition of various anions and bio-relative species at high concentrations (1 mM) (Fig. 3). Among the 15 additional analyte tested (Cl^-, I^-, CN^-,SCN^-, PO_4^{3-}, CO_3^{2-}, NO_2^-, NO_3^-, citrate, EDTA, boric acid, OH^-, $S_2O_3^{2-}$, S^{2-} and H_2O_2), very limited responses were observed. Considering that the azo group in **SP-2** might be reduced inside cells, some possible biological reducing agents, such as ascorbic acid, cysteine (Cys), homocysteine (Hcy), reduced glutathione (GSH), dithiothreitol (DTT), and 2-mercaptoethanol (BME), were also tested. Only a 3-fold enhancement in the phosphorescent intensity was observed at high concentrations (1 mM) of these bio-reducing agents. When 10 μM sulphite or bisulphite was added into an **SP-2** solution, the phosphorescent intensity increased significantly. These results suggest that **SP-2** is a sensitive and selective probe for sulphite/bisulphite detection.

Intracellular sulphite/bisulphite imaging

Inspired by the excellent sensing properties of **SP-2** for sulphite/bisulphite *in vitro*, we used this probe for tracing intracellular

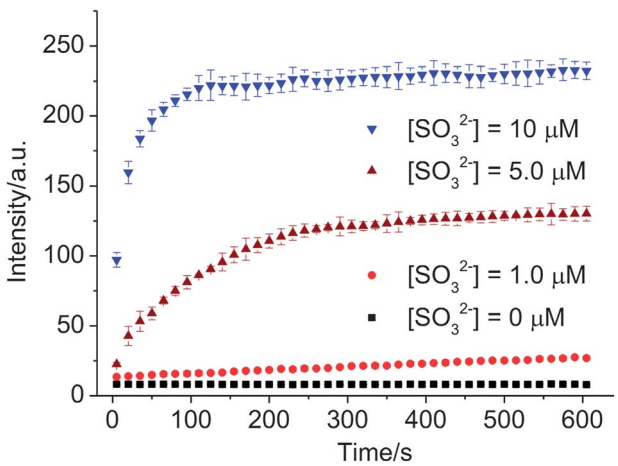

Fig. 2 Phosphorescence intensity of 10 μM **SP-2** treated with different concentrations of sulphite in a mixed solution of DMSO : HEPES buffer (3 : 7, 10 mM, pH 7.5) over time, $\lambda_{ex} = 405$ nm, $\lambda_{em} = 600$ nm.

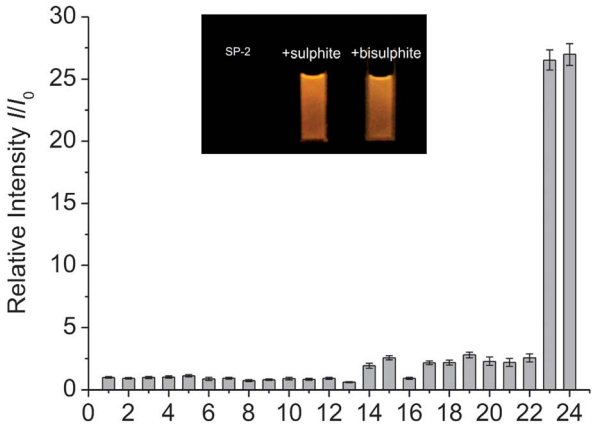

Fig. 3 Relative emission intensity of **SP-2** (10 μM) treated with different anions or reducing agents (1 mM of each species except for 10 μM of sulphite or bisulphite) in a mixed solution of DMSO : HEPES buffer (3 : 7, 10 mM, pH 7.5), $\lambda_{ex} = 405$ nm, $\lambda_{em} = 600$ nm. Bar (1) control, (2) Cl^-, (3) I^-, (4) CN^-, (5) SCN^-, (6) CO_3^{2-}, (7) NO_2^-, (8) NO_3^-, (9) citrate, (10) EDTA, (11) boric acid, (12) OH^-, (13) PO_4^{3-}, (14) $S_2O_3^{2-}$, (15) S^{2-}, (16) H_2O_2, (17) ascorbic acid, (18) Cys, (19) Hcy, (20) GSH, (21) DTT, (22) BME, (23) SO_3^{2-} and (24) HSO_3^-. Inset: visualisation of the phosphorescent response toward sulphite and bisulphite under a handheld 365 nm lamp.

sulphite/bisulphite. After 24 h of incubation with 5.0 μM **SP-2**, HepG2 cells exhibited a cellular viability greater than 88%, indicating that minimal adverse effects were induced by **SP-2** (ESI, Fig. S6†). HepG2 cells were incubated with increasing amounts of sulphite or bisulphite (10, 50, and 250 μM) for 1 h, the medium was replaced with PBS buffer, and the cells were incubated with 5.0 μM **SP-2** for an additional 1 h. The confocal microscope settings, including transmission density, brightness, contrast, and scan speed, were held constant to compare the relative intensity of the intracellular phosphorescence for all images. An off–on response of **SP-2** toward sulphite or bisulphite was also observed inside the HepG2 cells. The collected signal intensity increased significantly as the sulphite (Fig. 4) or bisulphite (ESI, Fig. S7†) concentrations increased from 10 to 250 μM. Higher concentrations of sulphite (or bisulphite) were required to generate a significant response toward **SP-2** for the living cell imaging experiments than were required for the *in vitro* assays. We reasoned that Na_2SO_3 and $NaHSO_3$, with their high charge density, could have difficulty passing through the cell membrane.

Endogenous sulphite/bisulphite response for SP-2

The high selectivity and sensitivity for exogenous sulphite and bisulphite detection by **SP-2** in both *in vitro* assays and in living cell imaging experiments encouraged us to test the response of this probe toward endogenous sulphite and bisulphite. Biological sulphite can be produced endogenously from thiosulphate *via* thiosulphate sulphurtransferase (TST) and can then be converted to sulphate *via* sulphate oxidase in mammals.[6,22] TST is one of two isoenzymes of rhodanese which is a mitochondrial enzyme that is widely distributed in nature and is especially abundant in mammalian livers.[23] TST first reacts with thiosulphate to yield a sulphur-substituted form of

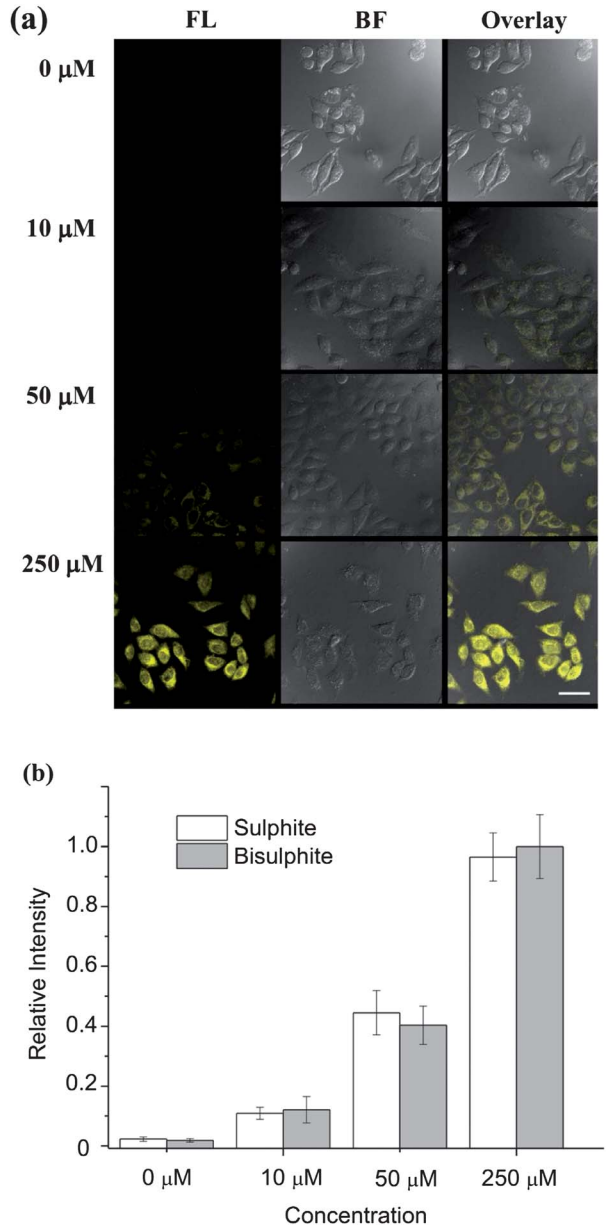

Fig. 4 (a) HepG2 cells were incubated for 1 h with increasing concentrations of sulphite (0–250 μM), and then the medium was replaced with PBS buffer and incubated with 5.0 μM **SP-2** for another 1 h. Confocal luminescence images were captured under excitation of a 405 nm laser. The scale bar represents 50 μm. (b) Normalized signal intensity collected in cells. The data represent the means ± s.d. of three independent experiments.

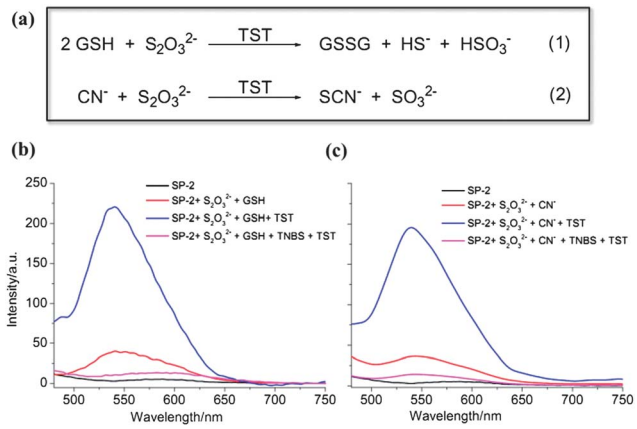

Fig. 5 (a) The enzymatic generation of sulphite or bisulphite by TST. A solution of 20 mM GSH (b) or 10 mM CN^- (c) was incubated with 10 μM **SP-2** and thiosulphate (10 mM) in PBS buffer containing 0.3% DMSO at 37 °C. Then, human TST-6* His fusion protein (15 μg mL^{-1}) was added, and the emission spectra were measured at 405 nm excitation.

the enzyme. Next, the enzyme-bound sulphur is transferred to a thiophilic acceptor, such as cyanide or GSH, to form thiocyanate or disulphide with the concomitant formation of sulphite or bisulphite (Fig. 5a). This reaction is important for the decontamination of cyanide because the thiocyanate formed is relatively harmless. However, TST is inactivated by 2,4,6-trinitrobenzenesulphonate (TNBS).[24]

Bisulphite that was enzymatically generated by TST was readily detected by combining GSH, thiosulphate, and TST. GSH alone (Fig. 3, bar 20) or GSH with added thiosulphate in PBS buffer incubated at 37 °C led to a limited increase in the phosphorescence intensity of **SP-2**. However, when GSH, thiosulphate, and TST were combined together and incubated at 37 °C for 10 min, the phosphorescence intensity increased significantly (Fig. 5b). When TST was pre-treated with 100 mM TNBS solution and then **SP-2**, thiosulphate and GSH were added and further incubated for 10 min, the phosphorescence signal response was found to be faint. In addition, the enzymatically generated sulphite by thiosulphate and CN^- mixture *via* TST could also induce an increase in phosphorescence intensity of **SP-2** (Fig. 5c). (**Caution**, CN^- is highly toxic and must be handled with great care!). This reaction could also be blocked by TNBS. Therefore, this probe can detect the biosynthesised sulphite and bisulphite.

In the next step, we tested whether **SP-2** could be used for the determination of endogenous sulphite and bisulphite inside living cells. Thiosulphate can be converted to sulphite or bisulphite by TST in the presence of CN^- or GSH. Therefore, the addition of thiosulphate and CN^- (or GSH) could result in an increased cellular concentration of sulphite (or bisulphite). The cellular imaging experiments were conducted with **SP-2** as previously described. HepG2 cells that were incubated with GSH, CN^-, SCN^- or TNBS solution alone showed a minimal phosphorescence signal, and cells that were incubated with thiosulphate alone exhibited a slight increase in signal intensity (Fig. 6B and ESI, Fig. S8†), whereas cells that were incubated with thiosulphate/GSH or thiosulphate/CN^- showed a significant response in cells (Fig. 6). These results indicated that the supplementation of thiosulphate/GSH or thiosulphate/CN^- led to an increased level of bisulphite or sulphite inside the cell and that **SP-2** responded accordingly. In contrast, when cells were pre-incubated with 100 mM TNBS solution for 2 h to inactivate TST activity and then incubated with **SP-2**, thiosulphate and CN^- or GSH, the cells showed very weak phosphorescence intensity. Thus, **SP-2** is capable of detecting not only external sulphite/bisulphite supplemented into cell cultures but also endogenous sulphite and bisulphite biosynthesised by enzymes inside the cells.

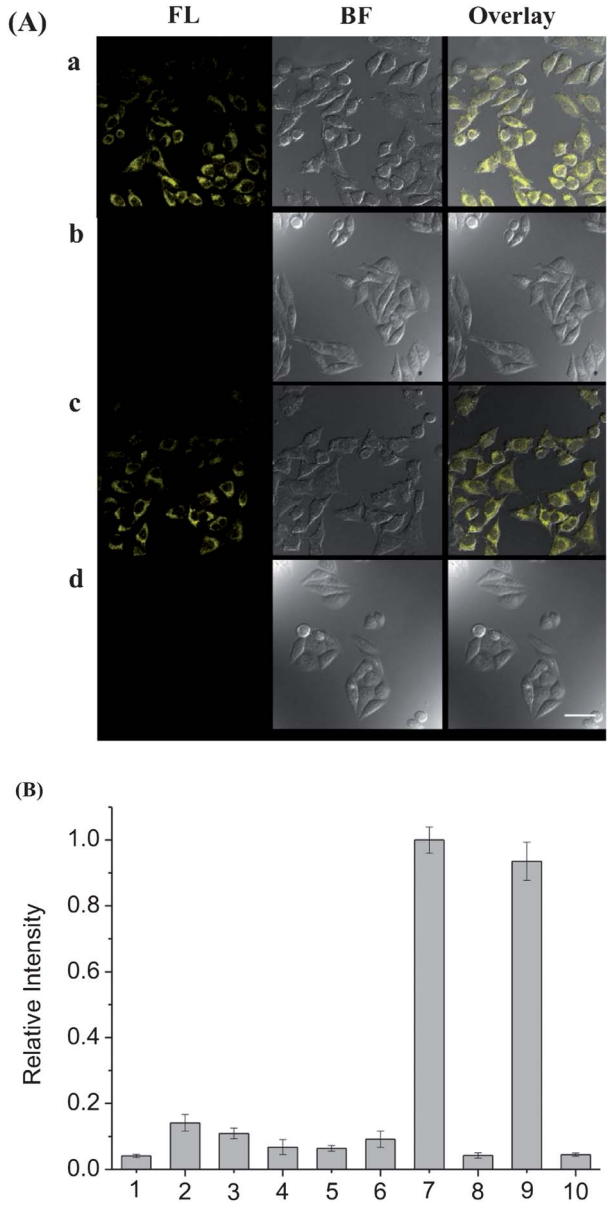

Fig. 6 (A) HepG2 cells were incubated for 1 h with 250 μM CN^-/250 μM thiosulphate (a) or 500 μM GSH/250 μM thiosulphate (c), then replaced with PBS buffer and incubated with 5.0 μM **SP-2** for another 1 h. For the control experiments, 100 mM TNBS solution was pre-incubated with hepG2 cells for 2 h (b) and (d). Confocal luminescence images were captured under excitation of a 405 nm laser. The scale bar represents 50 μm. (B) Normalized signal intensity collected in cells. Bar (1) control, **SP-2** alone; (2) $Na_2S_2O_3$, (3) GSH, (4) CN^-, (5) SCN^-, (6) TNBS, (7) CN^- + $Na_2S_2O_3$; (8) TNBS + CN^- + $Na_2S_2O_3$; (9) GSH + $Na_2S_2O_3$; (10) TNBS + GSH + $Na_2S_2O_3$. The data represent the means ± s.d. of three independent experiments.

Mechanism

We reasoned that the destruction of the azo group was responsible for the increase in phosphorescence intensity, and cyclic voltammetry was performed to verify the speculation. As shown in Fig. S9 (ESI),† **SP-2** showed reduction waves at potentials of −0.23 V ($\varphi_{azo0/-1}$) and −0.75 V ($\varphi_{azo-1/-2}$) in CH_3CN solution. Upon the addition of sulphite, both the reduction waves of $azo^{0/-1}$ and $azo^{-1/-2}$ disappeared. This result confirmed that the azo moiety in **SP-2** is the recognition site of the reaction to sulphite. To identify the reaction product, **SP-2** was reacted with sulphite and then isolated, purified, and further characterised using ESI-MS, XPS, FT-IR and ^1H NMR.

The high-resolution mass spectrum (HRMS) was conducted by zoom-scanning the iridium isotope peaks. The mass spectrum of the starting **SP-2** ($C_{64}H_{46}N_{10}Ir_2$) showed a bivalence peak at 670.2, corresponding to $[\mathbf{SP\text{-}2}]^{2+}$ (ESI, Fig. S10†). After reaction with sulphite, the sulphite-conjugated product was formed, as shown by the appearance of a peak at 1421.2 calcd. for $C_{64}H_{47}N_{10}Ir_2SO_3$. A sulphite-discharged fragment, which was ionised under the mass spectrometry conditions, was also formed as shown by the peak at 1341.3 calcd. for $C_{64}H_{47}N_{10}Ir_2$. The HRMS results matched perfectly with the simulation (Fig. 7). These results suggested the sulphite addition reaction mechanism (Scheme 2).

To verify this hypothesis, X-ray photoelectron spectra (XPS) were tested (Fig. 8). The XPS data showed no peak for the S 2p core-level of **SP-2**. After reaction with sulphite, however, in isolated product the S 2p core-level peak was present at approximately 168.60 eV binding energy, suggesting an S(VI) core.[25] Furthermore, the N 1s core-level XPS of the isolated product was shifted to lower binding energy from 400.50 to 400.05 eV compared to **SP-2**, which might be attributed to a more negative N than that in the azo bond.[26] The appearance of S(VI) and the destruction of the azo bond in the isolated product strongly supported the addition reaction mechanism between **SP-2** and sulphite. In the FT-IR spectrum, the isolated product exhibited enhanced absorption peaks at 1258 cm^{-1} and 1035 cm^{-1}, which are the absorption peaks of S–O in a sulphite conjugate. A moderate, sharp peak at 3360 cm^{-1}, attributable to N–H absorption, was also observed (ESI, Fig. S11†). In the ^1H NMR spectrum of the isolated product, a broad peak at 8.34 ppm with one ^1H integral was observed and it was not related with any of the ^{13}C NMR peaks in the ^{13}C–^1H COSY (ESI, Fig. S12, S13†). These results suggested that this broad peak corresponded to the N–H peak. This broad peak could not be exchanged by deuteroxide, which we speculated was due to the intramolecular hydrogen bond between the oxygen atom in S–O and the hydrogen atom in N–H. Because the N–H proton signal was stable in deuteroxide, a ^1H NMR titration experiment was performed to give detailed information (ESI, Fig. S14†). Therefore,

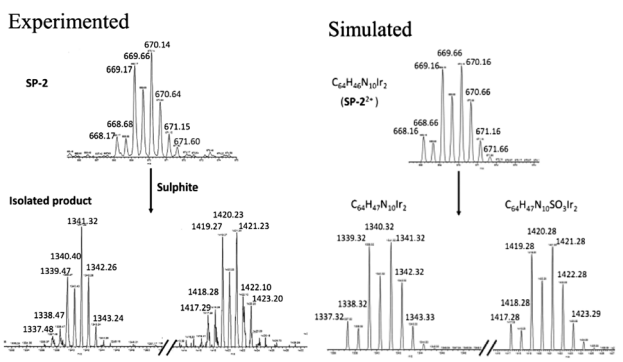

Fig. 7 HRMS of **SP-2** and its product after reaction with sulphite.

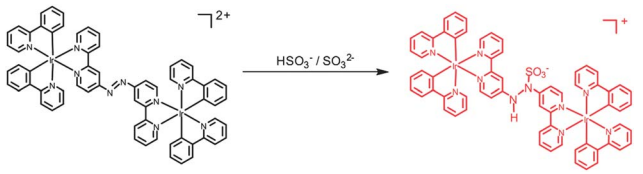

Scheme 2 Reaction of **SP-2** with sulphite or bisulphite.

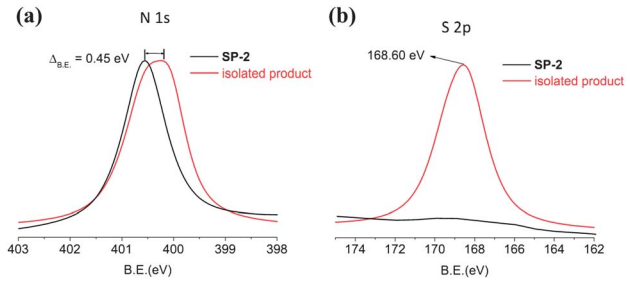

Fig. 8 XPS of **SP-2** and its product after reaction with sulphite.

we can conclude that the azo group in **SP-2** is conjugated with sulphite and participates in a sulphite-addition mechanism.

Conclusion

In summary, we have successfully developed a chemical strategy for sulphite/bisulphite selective probing both *in vitro* and in living cells. An azo group-bridged dinuclear iridium(III) complex, **SP-2**, was developed as a sulphite/bisulphite probe and showed a highly selective and sensitive response to sulphite/bisulphite with a detection limit of approximately 0.2 μM *in vitro*. This probe is suitable for live-cell imaging and can detect not only extraneous sulphite/bisulphite supplemented in cell cultures but also endogenously generated sulphite/bisulphite inside living cells. This strategy can be readily adapted for the design of new probes for biological SO_2 (sulphite/bisulphite) by changing the auxiliary C–N ligands.

Studies of biological gaseous SO_2 and its derivatives are ongoing and suggest that they play an important role in the cardiovascular system at physiological concentrations. The conjecture regarding whether SO_2 acts as a potential gasotransmitter[7,27] is still under discussion. A new method to analyse biological SO_2 and its derivatives in real-time could help to elucidate pathways for SO_2 production and make it possible to discover new roles for SO_2 derivatives in biological systems. Further optimisation and utilisation of this strategy for the design of new SO_2 derivative probes should dramatically accelerate further studies of SO_2 and its derivatives.

Experimental

Materials

Unless otherwise mentioned, all chemical reagents and solvents were purchased from commercial suppliers and used without further purification. Solvents were purified by standard methods prior to use. Human TST-6* His fusion protein was purchased from ProteinTech Group, Inc., Chicago (Genbank no. BC010148) and was used without further purification. Twice-distilled water was used throughout all experiments. HEPES buffer (10 mM) was prepared as follows: 2.383 g HEPES, 1000 mL H_2O, pH 7.5.

Instruments

Microanalysis (C, H and N) was performed with a Vario EL elemental analyser. Electrospray mass spectra were recorded on an LCQ system (LCQ DECA XP, Thermo Fisher Scientific, USA). ^{1}H NMR spectra were recorded on a Bruker AVANCE 400 Superconducting Fourier Transform Nuclear Magnetic Spectrometer. All chemical shifts were given relative to tetramethylsilane (TMS). FT-IR spectra were recorded on a Bruker VECTOR22 spectrometer in KBr pellets over a range of 400–4000 cm^{-1}. UV-Vis spectra were recorded on a Perkin-Elmer Lambda 850 spectrophotometer. Emission spectra were recorded on a Perkin-Elmer L55 spectrofluorophotometer. Cyclic voltammetry measurements were performed on a CHI 660A electrochemical workstation. All samples dissolved in CH_3CN were purged with Ar, and 0.1 M tetrabutylammonium perchlorate (TBAP) was used as a supporting electrolyte. A standard three-electrode system comprising a glassy carbon working electrode, a Pt-wire auxiliary electrode and a saturated calomel reference electrode (SCE) was used. The scan rate was 0.1 V s^{-1}. The pH measurements were conducted with a Sartorius PB-10 pH-meter. The XPS measurements were performed on an ESCALAB 250 spectrometer (Thermo Fisher Scientific, USA) equipped with a monochromatised Al Kα X-ray source (1486.6 eV photons).

Synthesis

The compounds $[Ir_2(ppy)_4Cl_2]$[19] and 4,4′′-azobis(2,2′-bipyridine) (azobpy)[20] were synthesised according to literature methods.

$[Ir(ppy)_2(azobpy)]PF_6$ (SP-1). A solution of $[Ir_2(ppy)_4Cl_2]$ (54 mg, 0.05 mmol) in $CHCl_3$ (15 mL) was added dropwise to a refluxing suspension of azobpy (68 mg, 0.2 mmol) in 15 mL of a $CHCl_3/CH_3OH$ (1 : 1) mixture. After 2 h, a solution of NH_4PF_6 (100 mg) in 2 mL of CH_3OH was added, and the mixture was refluxed for 30 min. The solvent was removed under reduced pressure. The precipitate was extracted with $CHCl_3$ and evaporated. The crude product was purified by neutral alumina with $CHCl_3/CH_3OH$ (30/1, v/v) as the eluent. Yield 85 mg, 87%. Anal. calcd. for $C_{42}H_{30}N_8F_6PIr$ (%): C, 51.27; H, 3.07; N, 11.39. Found (%): C, 51.19; H, 3.06; N, 11.46. ES-MS (CH_3OH) *m*/*z*: 838.3 [M-PF_6^-]$^+$. ^{1}H NMR (400 MHz, CD_3CN-d_3): δ 8.98 (s, 1H), 8.94 (d, J = 5.4 Hz, 1H), 8.84 (s, 1H), 8.71 (t, J = 6.4 Hz, 2H), 8.47 (d, J = 8.0 Hz, 1H), 8.18 (dd, J = 11.2, 6.4 Hz, 2H), 8.07 (d, J = 8.0 Hz, 2H), 8.01 (d, J = 4.8 Hz, 1H), 7.94 (t, J = 7.2 Hz, 1H), 7.90–7.77 (m, 6H), 7.69 (d, J = 5.4 Hz, 1H), 7.63 (d, J = 5.4 Hz, 1H), 7.55 (t, J = 8.0 Hz, 1H), 7.45 (t, J = 8.0 Hz, 1H), 7.10–6.98 (m, 4H), 6.93 (dd, J = 11.2, 7.2 Hz, 2H), 6.29 (t, J = 7.2 Hz, 2H).

$[Ir(ppy)_2(azobpy)Ir(ppy)_2](PF_6)_2$ (SP-2). A mixture of azobpy (34 mg, 0.1 mmol) and $[Ir_2(ppy)_4Cl_2]$ (108 mg, 0.1 mmol) was suspended in 20 mL of $CH_3OH/CHCl_3$ (1 : 1, v/v) and heated at 65 °C. After 4 h of reflux, 200 mg of NH_4PF_6 dissolved in 2 mL of CH_3OH was added to the mixture while stirring for another 30

min and then cooling to room temperature. The solvent was removed under reduced pressure. The precipitate was extracted with $CHCl_3$ and evaporated. The crude product was purified by column chromatography on neutral alumina with $CHCl_3$/CH_3OH (20/1, v/v) as the eluent. Yield: 89 mg, 55%. Anal. calcd. for $C_{64}H_{46}N_{10}F_{12}P_2Ir_2$ (%): C, 47.17; H, 2.85; N, 8.60. Found (%): C, 47.16; H, 2.91; N, 8.57. ES-MS (CH_3OH) *m*/*z*: 670.2 [M-$2PF_6^-$]$^{2+}$, 1483.0 [M-PF_6^-]$^+$. ^{1}H NMR (400 MHz, CD_3CN-d_3): δ 8.91 (s, 2H), 8.65 (d, J = 8.0 Hz, 2H), 8.23 (d, J = 6.0 Hz, 2H), 8.17 (t, J = 8.0 Hz, 2H), 8.06 (d, J = 8.4 Hz, 4H), 8.01 (d, J = 5.6 Hz, 2H), 7.83 (dd, J = 13.2, 6.8 Hz, 10H), 7.67 (d, J = 5.6 Hz, 2H), 7.61 (d, J = 5.6 Hz, 2H), 7.58–7.51 (m, 2H), 7.08–7.01 (m, 8H), 6.97–6.85 (m, 4H), 6.33–6.21 (m, 4H).

Sulphite conjugated product. SP-2. Sulphite conjugated product. **SP-2** (30 mg) was mixed with sodium sulphite (300 mg) in a CH_3CN/H_2O solution stirred at R.T. for 30 min, and then the solvent was removed. The solid was extracted with $CHCl_3$, washed with H_2O, and dried over Na_2SO_4. The solvent was removed under reduced pressure, and the product was further purified by column chromatography on neutral alumina with $CHCl_3/CH_3OH$ (20/1, v/v) as the eluent. Yield: 22 mg, 73%. ES-MS (CH_3OH) *m*/*z*: 1341.3, *m*/*z* = 1421.2. ^{1}H NMR (400 MHz, CD_3CN-d_3): δ 8.57 (d, J = 4.0 Hz, 1H), 8.41 (d, J = 8.0 Hz, 1H), 8.34 (br, 1H), 8.05 (d, J = 4.8 Hz, 6H), 7.95 (t, J = 8.0 Hz, 2H), 7.86–7.81 (m, 4H), 7.78 (dd, J = 7.2, 3.2 Hz, 4H), 7.71 (dd, J = 5.6, 3.2 Hz, 4H), 7.67–7.56 (m, 4H), 7.51 (dd, J = 13.2, 6.4 Hz, 1H), 7.47–7.40 (m, 2H), 7.32 (dd, J = 6.4, 2.4 Hz, 1H), 7.02 (dd, J = 13.2, 8.0 Hz, 8H), 6.94–6.81 (m, 4H), 6.26 (dd, J = 15.2, 7.2 Hz, 4H).

Cell viability assay

Hepatocellular carcinoma cell lines HepG2 were purchased from the American Type Culture Collection (ATCC, Manassas, VA). The cell lines were maintained in either RPMI-1640 or DMEM media supplemented with foetal bovine serum (10%), penicillin (100 units per mL) and streptomycin (50 units per mL) at 37 °C in a CO_2 incubator (95% relative humidity, 5% CO_2).

The cytotoxicity of **SP-2** was evaluated in HepG2 cells by the MTT assay[28] (MTT = 3-(4,5-dimethylthiazol-2-yl)-2,5-diphenyltetraazolium bromide). At 2–3 days after seeding, the cells were counted by a haemocytometer and seeded into a 96-well cell-culture plate at a cell density of 1×10^4 cells per well and were then incubated for 24 h at 37 °C under 5% CO_2. **SP-2** was then added at the indicated concentrations to quadruplicate wells. After 24 hours, the medium was replaced with fresh DMEM medium, and MTT was added to each well at a final volume of 0.5 mg mL^{-1}. The microplates were incubated at 37 °C for 4 h. The medium was then removed, and 100 μL of DMSO solution was added to the plates and shaken to dissolve the formazan products. The optical density of each well was then measured on a Tecan Infinite M200 monochromator-based multifunction microplate reader at a wavelength of 490 nm. The cell survival rate in the control wells without **SP-2** solution was considered to be 100% cell survival.

Cellular imaging experiments

The HepG2 cells were seeded at a density of 2×10^6 cells per mL of culture media. After 24 h, the cells were treated with or without sulphite or bisulphite, or other species in DMEM media for 1 h. After removing the DMEM media and washing with PBS to remove the remaining compounds, the HepG2 cells were further incubated with a 5.0 μM **SP-2** solution in PBS buffer for 1 h. Cell images were captured with a Leica TCS-SP5 confocal microscope (63× oil objective lens). The laser excitation wavelength was 405 nm, and the emission spectra were integrated over the range of 500–650 nm (single channel). For all images, the confocal microscope settings, such as transmission density, brightness, contrast, and scan speed were held constant to compare the relative intensity of intracellular phosphorescence.

Acknowledgements

This work was supported by the National Science of Foundation of China (no. 21071155, 21172273, 21171177, 91122010), Program for Changjiang Scholars and Innovative Research Team in University of China (no. IRT1298), the National Science Foundation of Guangdong Province (9351027501000003), the Research Fund for the Doctoral Program of Higher Education (20110171110013), the State Key Laboratory of Optoelectronic Materials and Technologies (2010-ZY-4-5) and Sun Yat-Sen University. We thank Dr Junhua Yao, Dr Shanyue Guan and Dr Wei Li for helping to design the analysis.

Notes and references

1 E. N. Schachter, T. J. Witek, G. J. Beck, H. Hosein, G. Colice, B. P. Leaderer and W. Cain, *Arch. Environ. Health*, 1984, **39**, 34–42.

2 W. Lee, K. Teschke, T. Kauppinen, A. Andersen, P. Jäppinen, I. Szadkowska, N. Pearce, B. Persson, A. Bergeret, L. A. Facchini, R. Kishi, D. Kielkowski, B. A. Rix, P. Henneberger, J. Sunyer, D. Colin, M. Kogevinas and P. Boffetta, *Environ. Health Perspect.*, 2002, **110**, 991–995.

3 C. S. Pundir and R. Rawal, *Anal. Bioanal. Chem.*, 2013, **405**, 3049–3062.

4 (*a*) R. Shapiro, *Mutat. Res., Rev.Genet. Toxicol.*, 1977, **39**, 149–175; (*b*) A. J. Ji, S. R. Savon and D. W. Jacobsen, *Clin. Chem.*, 1995, **41**, 897–903.

5 (*a*) H. Mitsuhashi, H. Ikeuchi, S. Yamashita, T. Kuroiwa, Y. Kaneko, K. Hiromura, K. Ueki and Y. Nojima, *Shock*, 2004, **21**, 99–102; (*b*) H. Kajiyama, Y. Nojima, H. Mitsuhashi, K. Ueki, S. Tamura, T. Sekihara, R. Wakamatsu, S. Yano and T. Naruse, *J. Am. Soc. Nephrol.*, 2000, **11**, 923–927.

6 (*a*) M. H. Stipanuk, J. D. Rosa and L. L. Hirschberger, *J. Nutr.*, 1990, **120**, 450–458; (*b*) H. Mitsuhashi, S. Yamashita, H. Ikeuchi, T. Kuroiwa, Y. Kanelo, K. Hiromura, K. Ueki and Y. Nojima, *Shock*, 2005, **24**, 229–234; (*c*) M. H. Stipanuk, *Annu. Rev. Nutr.*, 1986, **6**, 179–209.

7 (*a*) X. Wang, H. Jin, C. Tang and J. Du, *Eur. J. Pharmacol.*, 2011, **670**, 1–6; (*b*) X. Wang, H. Jin, C. Tang and J. Du, *Clin. Exp. Pharmacol. Physiol.*, 2010, **37**, 745–752.

8 Z. Meng, J. Li, Q. Zhang, W. Bai, Z. Yang, Y. Zhao and F. Wang, *Inhalation Toxicol.*, 2009, **21**, 1223–1228.
9 (*a*) M. K. Kim, C. S. Lim, J. T. Hong, J. H. Han, H. Y. Jang, H. M. Kim and B. R. Cho, *Angew. Chem., Int. Ed.*, 2010, **49**, 364–367; (*b*) Y. You, Y. Han, Y. Lee, S. Y. Park, W. Nam and S. J. Lippard, *J. Am. Chem. Soc.*, 2011, **133**, 11488–11491; (*c*) D. W. Domaille, L. Zeng and C. J. Chang, *J. Am. Chem. Soc.*, 2010, **132**, 1194–1195; (*d*) T. Hirayama, K. Okuda and H. Nagasawa, *Chem. Sci.*, 2013, **4**, 1250–1256.
10 (*a*) A. R. Lippert, E. J. New and C. J. Chang, *J. Am. Chem. Soc.*, 2011, **133**, 10078–10080; (*b*) Y. Qian, J. Karpus, O. Kabil, S. Zhang, H. Zhu, R. Banerjee, J. Zhao and C. He, *Nat. Commun.*, 2011, **2**, 495–501; (*c*) J. Wang, J. Karpus, B. S. Zhao, Z. Luo, P. R. Chen and C. He, *Angew. Chem., Int. Ed.*, 2012, **51**, 9652–9656; (*d*) Z. Q. Guo, S. Nam, S. Park and J. Yoon, *Chem. Sci.*, 2012, **3**, 2760–2765; (*e*) K. H. Xu, M. M. Qiang, W. Gao, R. X. Su, N. Li, Y. Gao, Y. X. Xie, F. P. Kong and B. Tang, *Chem. Sci.*, 2013, **4**, 1079–1086.
11 (*a*) M. R. Gill, J. Garcia-Lara, S. J. Foster, C. Smythe, G. Battaglia and J. A. Thomas, *Nat. Chem.*, 2009, **1**, 662–667; (*b*) X. Peng, T. Wu, J. Fan, J. Wang, S. Zhang, F. Song and S. Sun, *Angew. Chem., Int. Ed.*, 2011, **50**, 4180–4183; (*c*) C. Li, M. Yu, Y. Sun, Y. Wu, C. Huang and F. Li, *J. Am. Chem. Soc.*, 2011, **133**, 11231–11239; (*d*) M. K. Lee, J. Williams, R. J. Twieg, J. H. Rao and W. E. Moerner, *Chem. Sci.*, 2013, **4**, 220–225.
12 (*a*) Y. Yang, F. Huo, J. Zhang, Z. Xie, J. Chao, C. Yin, H. Tong, D. Liu, S. Jin, F. Cheng and X. Yan, *Sens. Actuators, B*, 2012, **166–167**, 665–670; (*b*) X. Yang, M. Zhao and G. Wang, *Sens. Actuators, B*, 2011, **152**, 8–13; (*c*) Y. Q. Sun, P. Wang, J. Liu, J. Zhang and W. Guo, *Analyst*, 2012, **137**, 3430–3433; (*d*) G. Wang, H. Qi and X. F. Yang, *Luminescence*, 2013, **28**, 97–101; (*e*) K. Chen, Y. Guo, Z. Lu, B. Yang and Z. Shi, *Chin. J. Chem.*, 2010, **28**, 55–60.
13 (*a*) X. Gu, C. Liu, Y. Zhu and Y. Zhu, *J. Agric. Food Chem.*, 2011, **59**, 11935–11939; (*b*) M. G. Choi, J. Hwang, S. Eor and S. K. Chang, *Org. Lett.*, 2010, **12**, 5624–5627; (*c*) S. Chen, P. Hou, J. Wang and X. Song, *RSC Adv.*, 2012, **2**, 10869–10873.
14 X. Cheng, H. Jia, J. Feng, J. Qin and Z. Li, *Sens. Actuators, B*, 2013, **184**, 274–280.
15 W. Lin, L. Long, L. Yuan, Z. Cao, B. Chen and W. Tan, *Org. Lett.*, 2008, **10**, 5577–5580.
16 Y. Sun, J. Liu, J. Zhang, T. Yang and W. Guo, *Chem. Commun.*, 2013, **49**, 2637–2639.
17 (*a*) J. Otsuki, K. Sato, M. Tsujino, N. Okuda, K. Araki and M. Seno, *Chem. Lett.*, 1996, 847–848; (*b*) J. Otsuki, K. Harada and K. Araki, *Chem. Lett.*, 1999, 269–270; (*c*) J. Otsuki, M. Tsujino, T. Iizaki, K. Araki, M. Seno, K. Takatera and T. Watanabe, *J. Am. Chem. Soc.*, 1997, **119**, 7895–7896; (*d*) S. Sun and A. J. Lees, *J. Am. Chem. Soc.*, 2000, **122**, 8956–8967; (*e*) G. Pourrieux, F. Fagalde, I. Romero, X. Fontrodona, T. Parella and N. E. Katz, *Inorg. Chem.*, 2010, **49**, 4084–4091.
18 Y. You and W. Nam, *Chem. Soc. Rev.*, 2012, **41**, 7061–7084.
19 S. Sprouse, K. A. King, P. J. Spellane and R. J. Watts, *J. Am. Chem. Soc.*, 1984, **106**, 6647–6653.
20 J. Otsuki, N. Omokawa, K. Yoshiba, I. Yoshikawa, T. Akasaka, T. Suenobu, T. Takido, K. Araki and S. Fukuzumi, *Inorg. Chem.*, 2003, **42**, 3057–3066.
21 Analytical Methods Committee, *Analyst*, 1987, **112**, 199–204.
22 R. Cipollone, P. Ascenzi, P. Tomao, F. Imperi and P. Visca, *J. Mol. Microbiol. Biotechnol.*, 2008, **15**, 199–211.
23 (*a*) J. H. Ploegman, G. Drent, K. H. Kalk and W. G. J. Hol, *Nature*, 1978, **273**, 124–129; (*b*) S. Ramasamy, S. Singh, P. Taniere, M. J. S. Langman and M. C. Eggo, *Am. J. Physiol.: Gastrointest. Liver Physiol.*, 2006, **23**, 288–296.
24 V. A. Malliopoulou, E. T. Rakitzis and T. B. Malliopoulou, *Anticancer Res.*, 1989, **9**, 1133–1136.
25 R. V. Siriwardane and J. M. Cook, *J. Colloid Interface Sci.*, 1986, **114**, 525–535.
26 (*a*) M. Camalli, F. Caruso, G. Mattogno and E. Rivarola, *Inorg. Chim. Acta*, 1990, **170**, 225–231; (*b*) M. Doring, M. Rudolph and E. Uhlig, *Z. Anorg. Allg. Chem.*, 1987, **554**, 217–226.
27 (*a*) Z. Meng and H. Zhang, *Inhalation Toxicol.*, 2007, **19**, 979–986; (*b*) N. D. Mathew, D. I. Schlipalius and P. R. Ebert, *J. Toxicol.*, 2011, **2011**, 394970; (*c*) J. L. Hart, *Front. Biosci.*, 2011, **3**, 736–749; (*d*) X. Li, F. W. Bazer, H. Gao, W. Jobgen, G. A. Johnson, P. Li, J. R. McKnight, M. C. Satterfield, T. E. Spencer and G. Wu, *Amino Acids*, 2009, **37**, 65–78.
28 T. R. Mosmann, *J. Immunol. Methods*, 1983, **65**, 55–63.